RSC Advances

ROYAL SOCIETY OF CHEMISTRY

www.rsc.org/advances

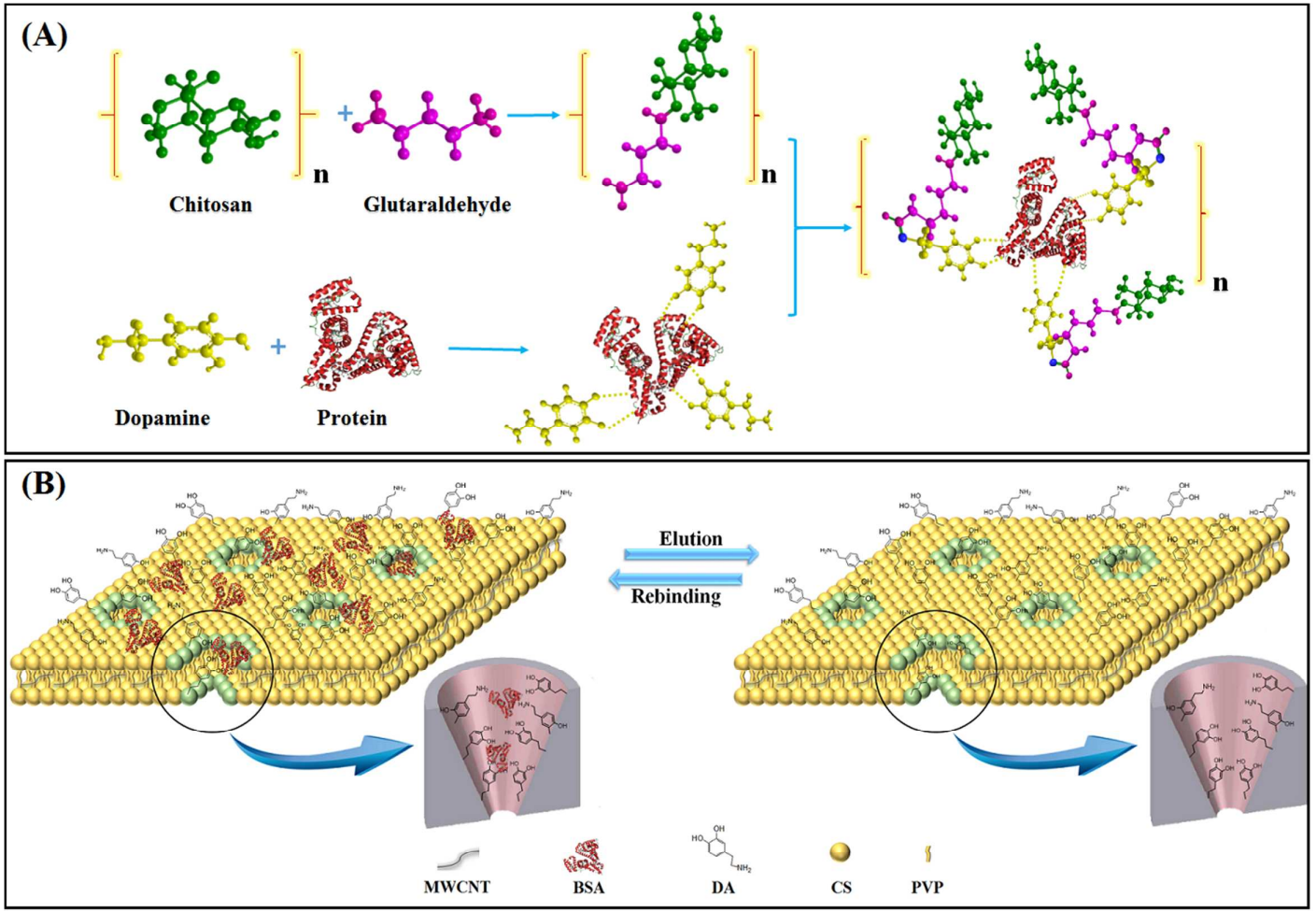

Graphical abstruct The proposed principle of polymerization of CP/CNT/DA-MIM (A) and the recognition protocol of CP/CNT/DA-MIM (B).

A porous hybrid imprinted membrane for selectively anchoring target proteins from a complex matrix

Zhimin Luo[a], Wei Du[a], Pengqi Guo[a], Penglei Zheng[a], Ruimiao Chang[a], Jin Wang[a], Aiguo Zeng[a], Chun Chang[a], Qiang Fu[a,*]

Abstract

A novel porous hybrid imprinted membrane (CP/CNT/DA-MIM) was prepared that could selectively anchor and separate target proteins from a complex matrix. CP/CNT/DA-MIM takes advantage of molecularly imprinted polymers and membranes, including the high selectivity of MIPs and the lower energy consumption and continuously separating mixtures of the membrane separation. The surface morphologies and physical/chemical properties of different membranes were investigated using FTIR, XRD, DSC, XPS and SEM. The results showed that the different molecules contained in CP/CNT/DA-MIM were homogeneous; two different sizes of imprinted cavities were observed in CP/CNT/DA-MIM that facilitate the selective anchoring property. The adsorption capacity, swelling behavior and mechanical properties of different constituent membranes were also compared. The results showed that the adhesion and nonspecific adsorption properties of the membrane were manifestly reduced by the addition of PVP. The binding capacity and adsorption selectivity of the membrane were apparently improved because of the existence of dopamine. MWCNTs obviously promoted the mechanical strength of the

[a] *School of Pharmacy, Xi'an Jiaotong University, 76 Yanta West Street, Xi'an, 710061, PR China*

* Corresponding author. Tel: +86 82655382; Fax: +86 82655382. *E-mail address*: fuqiang@mail.xjtu.edu.cn.

membranes. CP/CNT/DA-MIM was successfully applied to separate bovine serum albumin from bovine blood. CP/CNT/DA-MIM is an economical, hydrophilic and eco-friendly membrane and provides a promising separation material for the large-scale continuous selective separation of target proteins from a complex matrix in commercial applications.

Keywords: molecularly imprinting; hybrid membrane; anchoring target protein

1. Introduction

To further study the structure and function of living organisms at the molecular level, the research of proteomics and genomics has recently been widely developed.[1] With the development of proteomics research, it is essential to selectively recognize and separate target proteins from a complex matrix for industrial protein purification, basic biomedical research and clinical diagnostics.[2] However, the detection and separation of proteins are complicated processes because of their complicated three dimensional structures, lability and denaturation tendency.[3] Proteins that have significant biological functions are often low abundance proteins, which increases the difficulty of detection and separation.[4] Although antibodies have been the most widely used tools for capturing target proteins, the generation of antibodies is time-consuming and expensive, and many proteins are difficult to raise antibodies against.[5] Additionally, antibodies are produced by living cells, and it is occasionally difficult to control their quality.[6] Therefore, an ideal protein-capture agent should not only have high specificity but also be an economical, stable, robust, available and nonbiological material. In this respect, molecularly imprinted polymers (MIPs), also

called "antibody mimics," are considered to be promising and facile separation materials. MIPs exhibit a wonderful application potential in the field of the recognition of amino acids, proteins and nucleotide derivatives.[7]

MIPs are formed by the polymerization of a desired template and functional monomer with cross-linkers. After removing the template, a customized three-dimensional nanocavity is formed with complementary binding sites for the target.[8] MIPs can act as artificial antibodies and exhibit high selectivity towards the imprinted molecule.[9] The significant advantages of MIPs include easy preparation, predictable specific recognition, low cost, high chemical/physical stability, robustness and reusability, which enable MIPs to be applied in the areas of separation,[10] drug delivery,[11] chemical sensors,[12] catalysis,[13] phytoextraction,[14] biological analysis,[15] and so on. Their most extensively investigated application has been as separation materials for the analysis of various compounds, including drugs,[16] pesticides,[17] trace elements,[18] proteins[6] and nucleotides[19]. Particularly, molecularly imprinted membrane (MIM) separation technology has been widely used in the field of separation and purification, which takes advantage of membranes and MIPs, including the high selectivity of MIPs and the lower energy consumption and the continuous separating of the membrane separation mixtures.[20] These characteristics are helpful for a large-scale continuous separation operation, especially in industrial applications. Therefore, it is believed that MIM is one of the most promising materials in the separation and purification fields.

To date, molecular imprinting has been proven to be particularly successful for

low-molecular-weight compounds.[12-14] Although several imprinting techniques for creating protein MIPs have been developed,[1,2] protein imprinting still faces challenges due to the inherent properties of proteins, including their complicated physicochemical properties, large sizes, poor solubility, sensitivity to chemical process and the limited viability in organic solvents, which is usually essential for MIP formation.[21]

Chitosan (CS), which contains abundant amino and hydroxyl groups, has remarkable affinity to proteins.[22] CS is a linear hydrophilic polysaccharide derived from the deacetylation of chitin, which is one of the most plentiful natural biopolymers. CS has a relatively good film-forming ability and is eco-friendly and safe for humans and the environment.[23] Furthermore, it is a biocompatible and biodegradable material with attractive properties, including hydrophilicity, biocompatibility, nontoxicity and high permeability toward water.[24] These endow CS with a wide usage in molecular separation, wastewater treatment, packaging materials, artificial skin, cosmetics, bone substitutes, and so on.[25] Moreover, CS has been widely used as a supporter or functional monomer for the recognition and immobilization of proteins.[26,27] However, the specific adsorption of CS for target proteins is unsatisfactory because of the abundant functional groups in CS.[22] Additionally, the fragility, the uncontrollable porosity and the adhesive property of chitosan matrices limit the feasibility and practicability in membrane separation.[25] To overcome its disadvantages, CS is typically mixed with other compounds, such as polytetrafluoroethylene,[28] polyvinyl alcohol,[29] polycaprolactone,[30] polyvinyl

pyrrolidone (PVP),[31] agarose[32] and carbon nanotubes (CNT).[25] CS and PVP can form a homogeneous phase due to the strong hydrogen binding forces between the two types of molecules.[33] PVP is also biocompatible, non-toxic and easy to fabricate a membrane; it possesses relatively good lubricity and anti-adhesive properties.[34] Additionally, PVP has been shown to control the porosity, reduce the adhesion and improve the elasticity of chitosan structures.[35] Particular, the addition of CNT into a chitosan matrix can significantly increase the tensile modulus and strength.[25]

In this work, an imprinted hybrid membrane is examined that provides the merits of selectivity, economy, stableness and hydrophilicity for anchoring target proteins from biological samples (such as blood samples). The membrane was prepared using a mixture of chitosan and polyvinyl pyrrolidone as the supporter, dopamine and chitosan as the bi-functional monomers, polyethylene glycol as the porogen and bovine serum albumin (BSA) as the model template. To further improve the physic/chemical properties of the membrane, functionalized MWCNTs with multiple surface hydroxyl and carboxyl groups were added into the membranes. The mechanical properties and swelling behaviors of different membranes were compared. The surface morphologies and physical/chemical properties of different membranes were also investigated using Fourier transform infrared spectroscopy, X-ray diffraction, differential scanning calorimetry, X-ray photoelectron spectroscopy and a scanning electron microscope. The adsorption capacity and imprinted factor of different membranes were also studied. Then, the chitosan/polyvinyl pyrrolidone/multi walled carbon nanotube/dopamine molecularly imprinted

membrane (CP/CNT/DA-MIM) was applied as a separation matrix to anchor BSA from bovine blood.

2. Experimental Method

2.1 Materials and reagents

CS with a 90% degree of deacetylation (MW = 600 000 g/mol) PVP (MW = 1 300 000 g/mol) and polyethylene glycol (PEG, MW = 20000 g/mol) were purchased from Sinopharm Chemical Reagent Co., Ltd. MWCNTs were purchased from Beijing DK Nano Technology Co., Ltd.. Their diameter and length were approximately 20 - 30 nm and 10 - 20 μm, respectively. MWCNTs were purified by thermal oxidation (at 500 ℃ for 30 min in air) and acid treatment (refluxed in concentrated sulfuric acid and a nitric acid solution (1:3, v/v) for 12 h and washed with water) before use. Dopamine hydrochloride was obtained from J&K Scientific, Ltd. (China). Bovine serum albumin (BSA), human serum albumin (HSA) and lysozyme (Lyz) were obtained from Sigma-Aldrich. Glutaraldehyde (25% aqueous solution), absolute acetic acid (99%), sodium chloride (99.5%), sodium borohydride (98%) and other chemicals were purchased from Sinopharm Chemical Reagent Co., Ltd. Ultrapure water purified with a Milli-Q system (Millipore) was used in all of the experiments. The bovine blood sample was collected from the local slaughter house.

2.2 Preparation of hybrid membranes

The CP/CNT/DA-MIM was prepared by the phase inversion method. The proposed principle of polymerization is demonstrated in Fig. 1. Five milligrams of functional MWCNTs were dissolved in 20 mL of water and sonicated for 3 h to obtain

a uniform dispersion of the MWCNT solution. Then, 0.4 mL of acetic acid, 0.25 g of chitosan powder, 0.25 g of PVP, 0.1 g of PEG and 0.2 mL of glutaraldehyde (25%) were added one by one and consecutively stirred for 2 h. The mixer was labeled as A. BSA (0.75 μmol) was dissolved in 5 mL of a PBS solution (5 mM, pH = 7.0); then, 60 μmol of DA was added with consecutive stirring for pre-assembly for roughly 1 h, generating mixture B. Solutions A and B were mixed together and 0.2 mL of sodium borohydride (0.2 mol/L) was added. The mixture was stirred continuously for 2 h. The solution was cast on a clean glass plate (9 × 12 cm) and dried at 30 °C. Then, the dried sample was immersed into 4% sodium hydroxide for 3 h to neutralize the residue acetic acid, and washed with distilled water. The membrane was then boiled for 1 h in 300 mL of water to extract the porogen. It was washed with 100 mL of 5 mM phosphate buffer that contained 1 M NaCl (pH = 7.0) to remove the embedded template protein until no BSA was detected in the supernatant (using a RF-5301PC fluorescence spectrophotometer (SHIMADZU, Japan)). The membrane was subsequently rinsed with distilled water. After drying in air, CP/CNT/DA-MIM was stored in a desiccator. The proposed presentation and the anchoring protocol of CP/CNT/DA-MIM are shown in Fig. 2.

The chitosan/polyvinylpyrrolidone/MWCNTs/dopamine-non-molecularly imprinted membrane (CP/CNT/DA-NIM) was fabricated identically as the CP/CNT/DA-MIM membrane but without the template proteins. A chitosan/polyvinylpyrrolidone -molecularly imprinted membrane (CP-MIM) and a chitosan/polyvinylpyrrolidone/

dopamine-molecularly imprinted membrane (CP/DA-MIM) were also prepared for comparison. The preparation protocol of the membranes is shown in Table 1.

2.3 Characterization of membranes

The morphology of the membranes was observed by a TM-1000 Scanning Electron Microscope (SEM) (Hitachi, Japan) and a JEOL 7800F Field Emission Scanning Electron Microscope (FESEM) (Hitachi, Japan). The chemical compositions of the membranes were recorded on a Thermo Nicolet Nexus 330 FT-IR spectrometer (Madison, USA) with a scanning range from 400 to 4000 cm^{-1} at room temperature. The calorimetry measurements were made using a Mettler Toledo 822e Differential Scanning Calorimeter (DSC) (Mettler-Toledo Inc., USA). All membranes were grinded and tested in crimped aluminum pans at a heating rate of 10 °C/min under dry N_2 gas (25 mL/min) over a temperature range from 25 to 300 °C. The mechanical properties of the membranes (2.0 × 4.0 cm) were performed on an AG-I model mechanical testing apparatus (Shimadzu Co., Japan) with an elongation rate of 1 mm/min at room temperature. The crystalline structures of the membranes were analyzed by X-ray diffraction (XRD) (XRD-6100, Shimadzu Co., Japan) using Cu Kα radiation (λ = 0.154 nm) at 40 kV and 200 mA. For the chemical composition analysis, a Kratos Axis Ultra DLD X-ray photoelectron spectroscopy (XPS) (Kratos, US) device was used with a mono Al K α X-ray source operating at 150 W.

2.4 Swelling test

The swelling test of the composite membranes was studied before and after hydration. The weight of a dry membrane (1 × 1 cm) was taken as W_d. The dry

membrane was immersed in water for 1 h. The membrane was then removed and swept with a filter paper; the wet membrane (W_w) was subsequently weighed. The swelling degree W (%) of the membrane was calculated according to Equation 1.

$$W(\%) = \left(\frac{W_w - W_d}{W_d}\right) \times 100 \quad \text{Eq. 1}$$

2.5 Binding Capacity of Membranes

Single protein solutions were prepared by dissolving BSA, HSA or Lyz in a phosphate buffer solution (50 mM, pH = 7.0). The protein binding was conducted by soaking and gently shaking the membrane sample in 10 mL of a single protein solution with different concentrations at 25 °C. After 2 h, the membrane sample was removed from the solution and washed with 20 mL of phosphate buffer (5 min, 3 times). The membrane was then soaked and shaken in 10 mL of 10% SDS:acetic acid (1:1, v/v) for 2 h to elute the bound protein at 25 °C. The concentrations of the protein solution before and after was absorbed by the membrane were determined using a fluorescence spectrophotometer. The protein binding capacity (Q) was calculated according to Equation 2.

$$Q = \frac{(C_0 - C_f)v}{V} \quad \text{Eq.2}$$

where C_0 (μmol/mL) and C_f (μmol/mL) are the initial and final concentrations of protein in the solution, respectively; v (mL) is the total volume of the solution; and V(cm^3) is the volume of the membrane.

The imprinted factor (IF) of the membranes was calculated using the relationship given below.

$$IF = \frac{Q_{MIM}}{Q_{NIM}} \quad \text{Eq.3}$$

where Q_{MIM} and Q_{NIM} are the adsorption amount of molecularly imprinted membrane (MIM) and the non-imprinted membrane (NIM) for the target protein, respectively.

2.6 Sample analysis

To evaluate the applicability and separation of CP/CNT/DA-MIM, CP/CNT/DA-MIM was used to separate BSA from bovine blood samples. The bovine blood sample was diluted 100-fold with Tris-HCl (50 mM, pH = 7.0) and then treated with CP/CNT/DA-MIM for 2 h at 25 °C. Then, the adsorbed membrane was rinsed with 2 mL of water; 10% SDS:acetic acid (1:1, v/v) was applied for 2 h to elute the adsorbed protein. SDS-PAGE was employed to detect the diluted bovine blood sample, the diluted bovine blood sample after membrane treatment and the eluted sample.

3. Results and discussion

3.1 Optimization of the preparation conditions for membranes

The preparation process of the membranes was optimized by changing the crucial factors, including the mass ratio of CS to PVP and the amount of DA, MWCNTs and the template. The results are given in Table 1 and Fig. 3.

To control the adhesion and the porosity of the CS membrane, PVP was mixed with CS and CS/PVP (CP) served as the supporter in the matrix. Fig. 3 (A) depicts that CS and PVP were compatible and that the mixture of CS/PVP was a homopolymer due to the strong hydrogen binding forces between them. These results are in agreement with results from previous studies.[31] As shown in Table 1, with the

increase of the ratio of PVP in the mixture, the swelling degree and the adsorption capacity of the membranes gradually decreased, but the *IF* of the membranes increased accordingly. This likely occurred because the addition of PVP reduced the size of the inner pore of the CS membranes; therefore, the retaining property of the membranes was decreased. Meanwhile, the existence of PVP covered part of the functional groups of CS and then inhibited the nonspecific adsorption property of the membranes. The result was in accordance with the findings of Lim et al..[36] They studied the interconnectivity of CS/PVP scaffolds, which could be increased by increasing the PVP in the mixtures. However, the excess PVP could aggregate together and break the minute pore structures; then, the adsorption capacity and *IF* of the membrane were simultaneously shortened in CP-MIM4.

Fig. 3 shows the photographs of the different membranes with different transparency. Comparing Fig. 3 (A) with Fig. 3 (B), the color of CP/DA-MIM is darker than that of CP-MIM, indicating that DA was cross-linked with chitosan.[37] These results are important because the existence of DA significantly improved the adsorption capacity and imprinted factor of the membranes for target proteins (Table 1). DA has multifunctional groups (catechol and amine groups) and good hydrophilicity and biocompatibility properties; these merits make it appropriate for imprinting proteins.[38] Dopamine was preassembled with the target protein through a noncovalent interaction before polymerization. The unit of dopamine-protein was fixed in the matrix after polymerization, and the dopamine was covalently bound with CS through glutaraldehyde crosslinking. Then, a particular imprinting cavity was

formed in the membrane after eluting the template protein; meanwhile, dopamine was retained in the cavity as the specific recognition site, which provided the anchoring structure for the protein. Conversely, the excess DA self-polymerized together and blocked the proteins in and out of the pores, which resulted in the reduction of the adsorption capacity of CP/DA-MIM3 (Table 1).

The mechanical properties of a membrane are crucial in its performance; membranes should not only be flexible but also strong enough to be handled in practical application.[39] To verify the enhancement of MWCNTs for the mechanical properties of a CP membrane, membranes with different contents of MWCNTs were investigated. The tensile strength of all of the membranes was decreased after hydration, while the elongation was increased, as shown in Table 2. Fig. 3 shows that the transparency of the membranes decreased gradually with the increase of MWCNTs. The swelling degree of the membranes was also reduced significantly with the increase of MWCNTs (Table 1). These results are important because the tensile strength and elongation were simultaneously improved with the increase of MWCNTs, indicating that MWCNTs could extensively raise the mechanical properties of the membrane whether the membrane was dry or wet. However, the excessive addition of MWCNTs (reaching 1.5% of CS/PVP) resulted in the reduction of the swelling degree and adsorption capacity. Excessive addition might result from the excessive MWCNTs that filled the holes of the membrane, which influenced the water absorption and mass transfer of proteins into the membrane. In general, the optimized

membrane was obtained as CP/CNT/DA-MIM2, which owns the highest adsorption capacity, imprinted factor and relative superior mechanical strength.

3.2 Characterization of membranes

It is well known that the miscibility of the molecules in a blend of polymers can be judged by their morphology and/or the properties of their solid state, such as the crystalline state, the melting temperature, the glass transition temperature, the mechanical relaxation, and so on.[33] Consequently, the morphologies and physical/ chemical properties of membranes were characterized.

3.2.1 SEM and FESEM

Fig. 4 shows the SEM and FESEM images of the front and back side of CP/CNT/DA-MIM and its cross-section. It can be observed that the thickness of the membrane is approximately 100 μm and that the membrane has an asymmetric structure with three features: (1) the front side of the membrane is cruder than the back side (Fig. 4 A and B), which is in favor of the adsorption for templates onto the front side; (2) the funneled thru-holes are widely distributed onto the membrane (Fig. 4 A, B and D), which was left by the porogen. The upstream side of the funneled thru-hole is approximately 5-10 μm (Fig. 4 A1) and the downstream side is approximately 1-2 μm (Fig. 4 B1). The existence of the funneled thru-holes is a benefit for solute diffusion through the membrane; (3) it still exists in the inhomogeneous nano-holes inside the membrane (Figs. 4 C1 and E). Note that a higher porosity inside the membrane might help to improve the solute diffusion into the membrane and enhance the adsorption capacity of the membrane because the

adsorption sites were both on the surface and inside the membrane. The possible interaction between the imprinted cavity and the target proteins is shown in Fig. 4 F. In general, the overall porosity of the membrane increased the contact area and facilitated the adsorption of the membrane for target proteins. Fig. 4 C1 shows that the MWCNTs were dispersed inside the membrane and cross-linked with the matrix, which improves the mechanical strength of the membrane. The activation of the MWCNTs introduced hydroxyl and carboxyl groups onto the surface of the MWCNTs, which not only improved the water-solution and dispersibility of the MWCNTs but also facilitated crosslinking. The results are in line with the findings of Shieh et al..[40]

3.2.2 FT-IR

The FTIR spectra of CP/CNT/DA-MIM, CP-MIM and the activated MWCNTs are given in Supplementary information Fig. 1. The absorption peaks at approximately 3443 cm^{-1} (O-H or N-H), 1281 cm^{-1} (C-N) and 1101 cm^{-1} (-C-O-C-) were the characteristic peaks of CP-MIM (Supplementary information Fig. 1 (b)), and all of the peaks were also observed in CP/CNT/DA-MIM. As shown in Supplementary information Fig. 1 (a), the bands at 1580 cm^{-1} (the vibration of the benzene skeleton) and 683 cm^{-1} (the out-of-plane bending of C-H) were both attributed to the characteristic peaks of the phenyl group, indicating the existence of dopamine; the peak at 1646 cm^{-1} was attributed to the stretching and bending vibration of -C=N-, suggesting that dopamine was cross-linked with chitosan using glutaraldehyde. As seen in Supplementary information Fig. 1 (c), the absorption peaks at approximately 3418 cm^{-1} (O-H) and 1129 cm^{-1} (C-O) were the characteristic peaks

of the hydroxyl groups on the MWCNTs; however, these characteristic peaks were covered in CP/CNT/DA-MIM, indicating that the MWCNTs were successfully activated and were all immersed into the hybrid membrane. The observation in this study agrees well with the findings of Venkatesan et al.. [41]

3.2.3 XPS

XPS was applied to characterize the surface chemical composition of the membranes (Fig. 5 and 6). As shown in Fig. 5, it was calculated that the C/N atomic ratio in CP-MIM is 9.8, close to the theoretical value of 8.5. After adding MWCNTs into the membrane, the C/N atomic ratio of CP/CNT-MIM greatly increased (C/N = 26.6). The addition of dopamine reduced the atomic ratio of C and N in CP/CNT/DA-MIM (C/N = 19.5), suggesting that the MWCNTs and dopamine were well-wrapped and cross-linked into the membranes and that decreased loss occurred during the manufacturing procedure. Fig. 6 (A) shows that the peak at 284.8 eV originates from CS or PVP sp2 carbon atoms (C-C bond); however, the peak at 286.7 eV is attributed to the C-O-C bond in CS, and the peak located at 288.6 eV is due to the C=O bond in PVP.[42] In Figs. 5b and 6 (B), the content of the C-C bond is up to 58.6%, which might be attributed to the high-carbon structure of the multiwall carbon nanotube. Fig. 6 (C) illustrates that the peak at 286.0 eV is attributed to the C=N bond, which results from the intermolecular cross-linking polymer structure among chitosan, glutaraldehyde and dopamine.[43] The peak at 288.2 eV originates from the C-OH bond in chitosan or dopamine, and the content of the C-OH bond reaches up to 19.1%. In

general, the abundant functional groups and well-defined network are favorable to efficient protein imprinting and rebinding.

3.2.4 DSC

To achieve greater insight regarding the thermal behavior of the membrane, DSC measurements were performed, and the resulting thermograms are shown in Fig. 7 and Table 3. Any change in the physical properties in the polymer matrix from crosslinking can be reflected in the glass transition temperature (T_g), the melting temperature (T_m) or the degradation temperature (T_d).[44] The DSC thermogram of virgin chitosan shows a T_g, T_m and T_d of 79.5, 192.9 and 312.7 °C, respectively (Table 3). The result corresponds with the results of Rachipudi et al.[44] and He et al., [45] but it is quite different from the T_g of 203°C reported by Sakurai et al..[33] These results are likely attributable to the different molecular weight and deacetylation degree of CS or different procedure for DSC measurements. Fig. 7 (b, d and f) shows an increasing tendency that the endothermic peaks at approximately 187.6, 198.5 and 241.2°C were the T_m of CP-MIM, CP/CNT-MIM and CP/CNT/DA-MIM, respectively. Table 3 also shows that the T_d increased in order of CP-MIM, CP/CNT-MIM and CP/CNT/DA-MIM; the thermal stability of the membranes increased with the addition of MWCNTs and DA. However, it is difficult to clearly observe the T_g of these three membranes in the DSC curve. The result agrees with previous research.[45]

3.2.5 XRD

The crystalline properties of the membranes were analyzed with an X-ray diffractometer, as shown in Fig. 8. Two main peaks observed at 10.5° and 20.0°

correspond to the 020 and 110 planes, respectively, which are the characteristic peaks of chitosan.[35] They were also found in all of the membranes, confirming the presence of chitosan (Fig. 8 a, b and c). The diffraction peaks at 2θ = 26.4° and 43.4°, corresponding to the 111 and 100 planes, respectively, were typical Bragg peaks of pristine MWCNTs (Fig. 8 d).[46] However, there were no strong adsorption peaks observed for the MWCNTs in all of the membranes, suggesting that the incorporation of MWCNT did not significantly affect the crystalline structure of CS. The result shows agreement with previous studies,[35] possibly attributed to the lower amount of MWCNTs compared to chitosan. The results also suggest that MWCNTs were well-wrapped and dispersed into the membrane matrix.

3.3 Adsorption property

The adsorption curves of different membranes for BSA are shown in Fig. 9 (A). The results intuitively illustrate that the adsorption capacity of CP/DA-MIM and CP/CNT/DA-MIM are relatively close and that both capacities are greater than that of CP-MIM. This indicates that dopamine played an important role in improving the binding capacity of the membrane, and the addition of MWCNTs showed less impact on the adsorption capacity of the membrane. The adsorption isotherm curves of CP/CNT/DA-MIM and CP/CNT/DA-NIM are shown in Fig. 9 (B). The saturated adsorption capacity and imprinted factor of CP/CNT/DA-MIM for BSA were 0.726 μmol/cm^3 and 2.8, respectively. The imprinted factor of CP/CNT/DA-MIM for Lyz was 1.2, which was much lower than that of BSA (Fig. 9 (C)), indicating the specific selectivity of CP/CNT/DA-MIM for template protein. The similarity in size and

composition of the amino acid between BSA and HSA caused the CP/CNT/DA-MIM to show a certain selectivity for HSA (IF = 1.9), which was still lower than that for BSA. The results fully confirm that CP/CNT/DA-MIM shows high specificity for the target protein.

3.4 Sample analysis

To investigate its adsorption, CP/CNT/DA-MIM was used to separate BSA from bovine blood samples, and the results are shown in Fig. 10. After treatment with CP/CNT/DA-MIM, the intensity of the BSA band in the blood sample (100-fold) was significantly weaker (lane 2). Then, the BSA band appeared again in the eluted solution after treatment with SDS-acetic acid (10%) (lane 3). The results indicated that CP/CNT/DA-MIM could specifically anchor BSA in the bovine blood sample. Thus, CP/CNT/DA-MIM has potential value in practical applications.

4. Conclusions

CP/CNT/DA-MIM was prepared for the selective anchoring of target proteins in a complex matrix, and its preparation condition was optimized according to the adsorption capacity, imprinted factor and mechanical properties. FTIR, XRD, DSC, XPS, SEM and FESEM were used to study the morphologies and physical/chemical properties of CP/CNT/DA-MIM. The results of this study showed that the different molecules contained in CP/CNT/DA-MIM were uniformly dispersed and cross-linked together. The proper addition of PVP, MWCNTs and DA reduced the adhesion and nonspecific adsorption, enhanced the mechanical properties and improved the binding selectivity of the membrane, respectively. The applicability and separation

effectiveness of CP/CNT/DA-MIM was also evaluated, and it was successfully used for the separation of BSA from the bovine blood sample. The generated membrane provided an economical, stable and biocompatible material for the selective separation and purification of target proteins, which can overcome the disadvantages of conventional separation methods (such as generating antibodies), including those that are time-consuming, expensive and difficult to obtain. Additionally, CP/CNT/DA-MIM was prepared and completely applied in the aqueous phase or under a gentle circumstance, which perfectly overcame the deficiency of the conventional preparation method for the molecular imprinting of polymers. Such a nontoxic, biocompatible, hydrophilic and low cost membrane system could potentially be an outstanding separation material for the large-scale continuous selective separation of target proteins from a complex matrix in the application of industrial protein purification, basic biomedical research and clinical diagnostics.

Acknowledgements

This work was financially supported by the National Natural Science Foundation of China (No. 81173024 and No. 81227802), the China Postdoctoral Science Foundation Funded Project (No. 2014M562428) and the Shaanxi Health Department of Scientific Research Project (No. 2014D73). We are grateful to Dr Min Zhang for revising the paper.

References

1 R. Gao, X. Mu AND J. Zhang, Y. Tang, *J. Mater. Chem. B*, 2014, **2**, 783-792.

2 A. Nematollahzadeh, W. Sun, C. S. A. Aureliano, D. Lutkemeyer, J. Stute, M.

Abdekhodaie, A. Shojaei and B. Sellergren, *Angew. Chem. Int. Ed.*, 2011, **50**, 495-498.

3 Y. Yang, X. He, Y. Wang, W. Li and Y. Zhang, *Biosens. Bioelectron*, 2014, **54**, 266-272.

4 Z. Ding, S.W. Annie Bligh, L. Tao, J. Quan, H. Nie, L. Zhu and X. Gong, *Mat. Sci. Eng. C*, 2015, **48**, 469-479.

5 B. T. S. Bui and K. Haupt, *Anal. Bioanal. Chem.*, 2010, **398**, 2481-2492.

6 M. J. Whitcombe, I. Chianella, L. Larcombe, S. A. Piletsky, J. Noble, R. Porter and A. Horgan, *Chem. Soc. Rev.*, 2011, **40**, 1547-1571.

7 G. Vasapollo, R. D. Sole, L. Mergola, M. R. Lazzoi, A. Scardino, S. Scorrano and G. Mele, *Int. J. Mol. Sci.*, 2011, **12**, 5908-5945.

8 M. Yang, L. Liao, G. Zhang, X. Xiao, Y. Lin and C. Nie, *Anal. Bioanal. Chem.*, 2013, **405**, 7545-7551.

9 R. Gao, L. Zhang, Y. Hao, X. Cui and Y. Tang, *RSC Adv.*, 2014, **4**, 64514-64524.

10 W. Du, Q. Fu, G. Zhao, P. Huang, Y. Jiao, H. Wu, Z. Luo and C. Chang, *Food Chem.*, 2013, **139**, 24-30.

11 J. Yin, Y. Cui, G. Yang and H. Wang, *Chem. Commun.*, 2010, **46**, 7688-7690.

12 Y. Fuchs, O. Soppera and K. Haupt, *Anal. Chim. Acta*, 2012, **717**, 7-20.

13 J. Liu and G. Wulff, *Angew. Chem. Int. Ed.*, 2004, **43**, 1287-1287.

14 S. K. Tsermentseli, P. Manesiotis, A. N. Assimopoulou and V. P. Papageorgiou, *J. Chromatogr. A*, 2013, **1315**, 15-20.

15 Y. Hoshino, H. Koide, T. Urakami, H. Kanazawa, T. Kodama, N. Oku and K. J.

Shea, *J. Am. Chem. Soc.*, 2010, **132**, 6644-6645.

16 Z. Luo, A. Zeng, P. Zheng, P. Guo, W. Du, K. Du and Q. Fu, *Anal. Methods*, 2014, **6**, 7865-7874.

17 L. Meng, X. Qiao, J. Song, Z. Xu, J. Xin and Y. Zhang, *J. Agric. Food Chem.*, 2011, **59**, 12745-12751.

18 M. Shamsipur, H. R. Rajabi, S. M. Pourmortazavi and M. Roushani, *Spectrochim. Acta A*, 2014, **117**, 24-33.

19 L. Longo and G. Vasapollo, *Mini-Rev. Org. Chem.*, 2008, **5**, 163-170.

20 J. Fan, L. Li, Z. Tian, C. Xie, F. Song, X. Zhang and J. Zhu, *J. Membrane Sci.*, 2014, **467**, 13-22.

21 E. Verheyen, J. P. Schillemans, M. van Wijk, M. Demeniex, W. E. Hennink and C. F. van Nostrum, *Biomaterials*, 2011, **32**, 3008-3020.

22 B. Krajewska, *Enzyme Microb. Tech.*, 2004, **35**, 126-139.

23 X. Zheng, Q. Lian and H. Yang, *RSC Adv.*, 2014, **4**, 42478-42485.

24 S. Chen, Y. Wu, F. Mi, Y. Lin, L. Yu and H. Sung, *J. Control. Release*, 2004, **96**, 285-300.

25 S. Wang, L. Shen, W. Zhang and Y. Tong, *Biomacromolecules*, 2005, **6**, 3067-3072.

26 Y. Xia, T. Guo, M. Song, B. Zhang and B. Zhang, *Biomacromolecules*, 2005, **6**, 2601-2606.

27 Y. Xia, T. Guo, H. Zhao, M. Song, B. Zhang and B. Zhang, *J. Biomed. Mater. Res. A*, 2009, **90**, 326-332.

28 B. Haimovich, L. Difazio, D. Katz, L. Zhang, R. S. Greco, Y. Dror and A. Freeman,

J. Appl. Polym. Sci., 1997, **63**, 1393-1400.

29 A. Lejardi, R. Hernández, M. Criado, J. I. Santos, A. Etxeberria, J. R. Sarasua and C. Mijangos, *Carbohyd. Polym.*, 2014, **103**, 267-273.

30 A. R. Sarasam, R. K. Krishnaswamy and S. V. Madihally, *Biomacromolecules*, 2006, **7**, 1131-1138.

31 T. H. M. Abou-Aiad, K. N. Abd-El-Nour, I. K. Hakim and M. Z. Elsabee, *Polymer*, 2006, **47**, 379-389.

32 S. Sun, Y. Tang, Q. Fu, X. Liu, L. Guo, Y. Zhao and C. Chang, *Int. J Biol. Macromol.*, 2012, **50**, 1002-1007.

33 K. Sakurai, T. Maegawa and T. Takahashi, *Polymer*, 2000, **41**, 7051-7056.

34 B. Wang, X. Liu, Y. Ji, K. Ren and J. Ji, *Carbohyd. Polym.*, 2012, **90**, 8-15.

35 J. Venkatesan, B. Ryu, P. N. Sudha and S. K. Kim, *Int. J. Biol. Macromol.*, 2012, **50**, 393-402.

36 J. I. Lim, H. Im and W. K. Lee, *J. Biomat. Sci. Polym. E.*, 2015, **26**, 32-41.

37 H. Lee, S. M. Dellatore, W. M. Miller and P. B. Messersmith, *Science*, 2007, **318**, 426-430.

38 Z. Xia, Z. Lin, Y. Xiao, L. Wang, J. Zheng, H. Yang and G. Chen, *Biosens. Bioelectron.*, 2013, **47**, 120-126.

39 P. I. Morgado, P. F. Lisboa, M. P. Ribeiro, S. P. Miguel, P. C. Simoes, I. J. Correia and A. Aguiar-Ricardo, *J. Membrane Sci.*, 2014, **469**, 262-271.

40 Y. T. Shieh and Y. F. Yang, *Eur. Polym J.*, 2006, **42**, 3162-3170.

41 P. N. Venkatesan and S. Dharmalingam, *J. Membrane Sci.*, 2013, **435**, 92-98.

42 Y. Pan, H. Bao and L. Li, *ACS Appl. Mater. Interfaces*, 2011, **3**, 4819-4830.

43 B. Ge, Y. Tan, Q. Xie, M. Ma and S. Yao, *Sensor. Actuat. B-Chem.*, 2009, **137**, 547-554.

44 P. S. Rachipudi, A. A. Kittur, A. M. Sajjan and M. Y. Kariduraganavar, *J. Membrane Sci.*, 2013, **441**, 83-92.

45 L. He, L. Yao, D. Yang, Q. Cheng, J. Sun, R. Song and Y. Hao, *J. Macromol. Sci. B*, 2011, **50**, 2454-2463.

46 Y. Hu, J. Li, Z. Zhang, H. Zhang, L. Luo and S. Yao, *Anal. Chim. Acta*, 2011, **698**, 61-68.

Table 1 Optimization of preparation conditions for membranes and their swelling degree, adsorption capacity and imprinted factor

Membranes	MWCNTs (%)	CS:PVP	BSA (μmol)	DA (μmol)	Swelling degree (%)	*Q* (μmol/cm^3)	*IF*
CP-MIM1	/	**5:1**	0.75	/	256.8±4.1	0.590±0.018	1.42±0.07
CP-NIM1	/	**5:1**	/	/	255.3±5.6	0.415±0.034	/
CP-MIM2	/	**5:3**	0.75	/	225.0±3.9	0.493±0.031	1.73±0.06
CP-NIM2	/	**5:3**	/	/	227.9±7.2	0.285±0.017	/
CP-MIM3	/	**5:5**	0.75	/	215.4±4.6	**0.459**±0.011	**1.81**±0.08
CP-NIM3	/	**5:5**	/	/	226.7±6.7	0.254±0.028	/
CP-MIM4	/	**5:7**	0.75	/	211.3±4.8	0.204±0.043	1.29±0.17
CP-NIM4	/	**5:7**	/	/	231.6±3.5	0.158±0.022	/
CP/DA-MIM1	/	5:5	0.75	**30**	203.0±2.9	0.557±0.031	2.06±0.15
CP/DA-NIM1	/	5:5	/	**30**	199.7±5.2	0.270±0.019	/
CP/DA-MIM2	/	5:5	0.75	**60**	185.3±3.4	**0.719**±0.017	2.75±0.06
CP/DA-NIM2	/	5:5	/	**60**	190.4±4.4	0.261±0.013	/
CP/DA-MIM3	/	5:5	0.75	**120**	196.2±4.1	0.505±0.024	1.86±0.09
CP/DA-NIM3	/	5:5	/	**120**	188.7±3.9	0.271±0.014	/
CP/CNT/DA-MIM1	**0.5**	5:5	0.75	60	191.1±2.7	0.711±0.018	2.68±0.11
CP/CNT/DA-NIM1	**0.5**	5:5	/	60	201.3±6.2	0.265±0.029	/
CP/CNT/DA-MIM2	**1**	5:5	0.75	60	182.5±4.9	**0.726**±0.012	2.76±0.06
CP/CNT/DA-NIM2	**1**	5:5	/	60	185.2±3.6	0.263±0.035	/
CP/CNT/DA-MIM3	**1.5**	5:5	0.75	60	165.2±5.4	0.433±0.038	2.01±0.15
CP/CNT/DA-NIM3	**1.5**	5:5	/	60	175.7±3.8	0.215±0.015	/
CP/CNT/DA-MIM4	1	5:5	**0.15**	60	185.4±6.3	0.395±0.026	1.50±0.12
CP/CNT/DA-MIM5	1	5:5	**1.5**	60	197.8±2.9	0.687±0.021	1.40±0.15

Table 2 The tensile strength and elongation at breaking of various membranes

	MWCNTs (%)	Tensile strength (N/mm^2)	Elongation (%)
Dry membranes	0	31.4	50%
	0.5	42.1	53%
	1	42.7	108%
	1.5	55.2	90%
Wet membranes	0	3.0	105%
	0.5	4.6	243%
	1	5.2	227%
	1.5	7.1	205%

Table 3 The values of T_g, T_m and T_d of chitosan, polyvinyl pyrrolidone, dopamine and membranes with different composition.

Sample	T_g	T_m	T_d
CS	79.5	192.9	312.7
PVP	52.4	192.4	>400
DA	/	249.8	347.6
CP-MIM	/	187.6	300.9
CP/CNT-MIM	/	198.5	316.5
CP/CNT/DA-MIM	/	241.2	320.0

Figure captions:

Fig. 1 The proposed principle of polymerization of CP/CNT/DA-MIM.

Fig. 2 The proposed presentation and the recognition protocol of CP/CNT/DA-MIM.

Fig. 3 The photographs of the membranes with different amounts of MWCNTs. A: CP-MIM3 (0%); B: CP/DA-MIM2 (0%); C: CP/CNT/DA-MIM1 (0.5%); D: CP/CNT/DA-MIM2 (1%); E: CP/CNT/DA-MIM3 (1.5%).

Fig. 4 SEM and FESEM images of the front (A, A1) and back side (B, B1) of CP/CNT/DA-MIM, the cross-section (C, C1) of the membrane with different magnification, the model of funneled thru-hole (D), binding sites (E) and imprinted cavity (F).

Fig. 5 XPS spectra of CP-MIM (a), CP/CNT-MIM (b) and CP/CNT/DA-MIM (c).

Fig. 6 XPS spectra of C 1s for (A) CP-MIM, (B) CP/CNT-MIM and (C) CP/CNT/DA-MIM.

Fig. 7 DSC curves of CS (a), CP-MIM (b), PVP (c), CP/CNT-MIM (d), DA (e), CP/CNT/DA-MIM (f).

Fig. 8 XRD curves of CP/CNT/DA-MIM (a), CP/CNT-MIM (b), CP/CNT-NIM (c) and virgin MWCNT (d).

Fig. 9 (A) Fluorescence spectrum of BSA before and after absorbed by different membranes; (B) Adsorption isotherm curves of CP/CNT/DA-MIM and CP/CNT/DA-NIM; (C) Adsorption capacity and imprinted factor of membranes for different substrates.

Fig. 10 SDS-PAGE analysis. Lanes 1, bovine blood diluted 100-fold; lanes 2, bovine blood sample (diluted 100-fold) after treated with CP/CNT/DA-MIM; lanes 3, the eluted solution; land 4, 0.25 $mg \cdot mL^{-1}$ of standard BSA solution; lane 5, standard weight molecular protein markers.

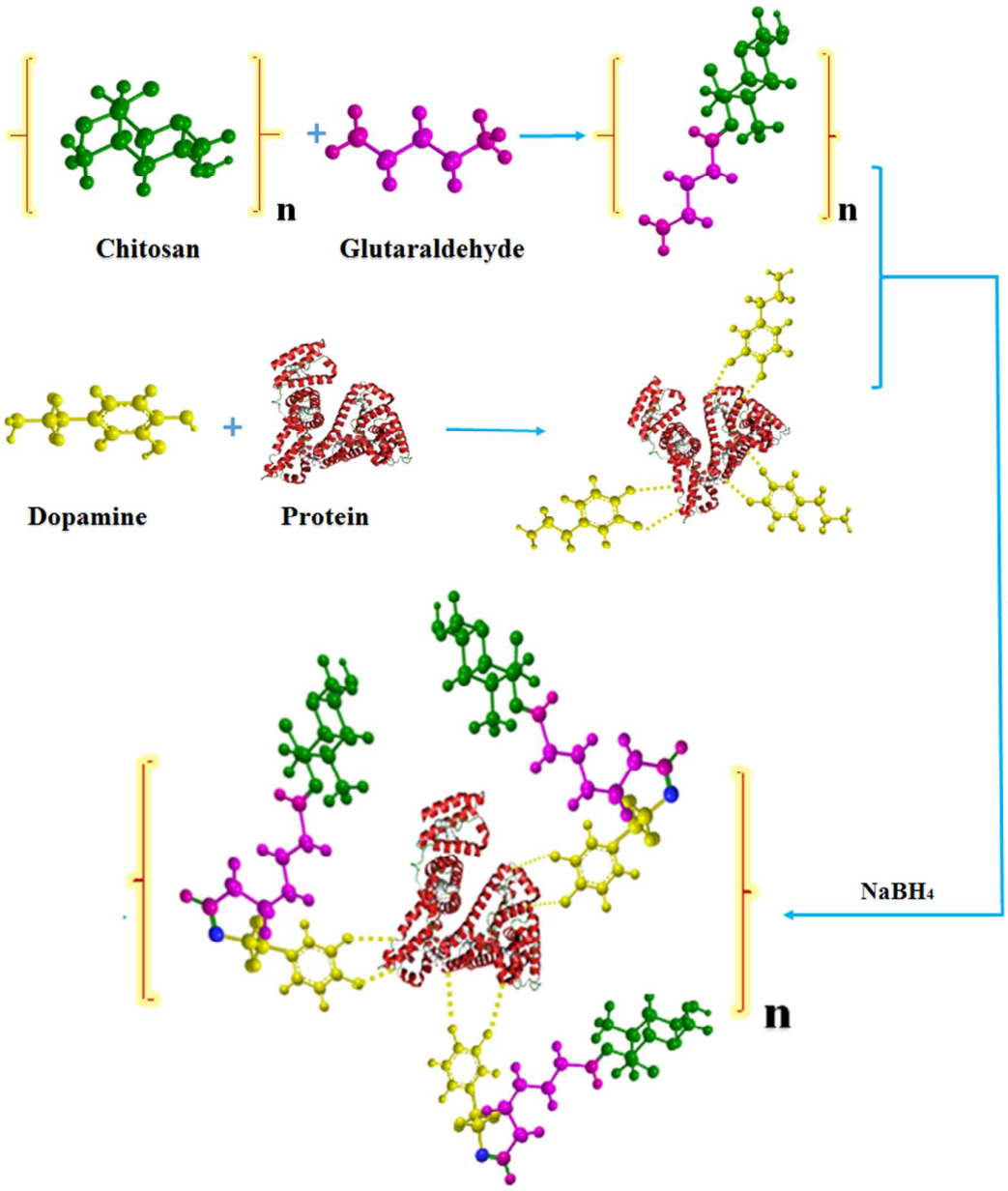

Fig. 1 The proposed principle of polymerization of CP/CNT/DA-MIM.

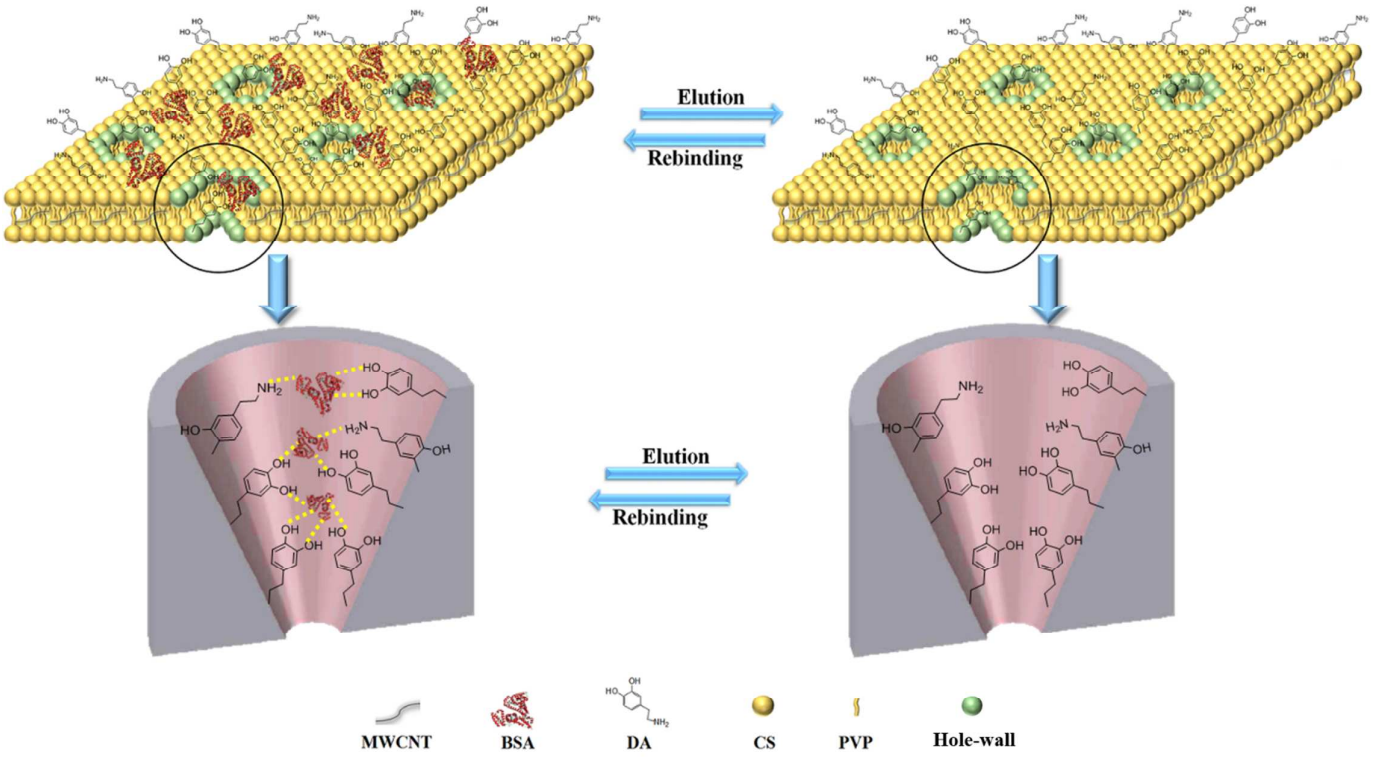

Fig. 2 the proposed presentation and the recognition protocol of CP/CNT/DA-MIM.

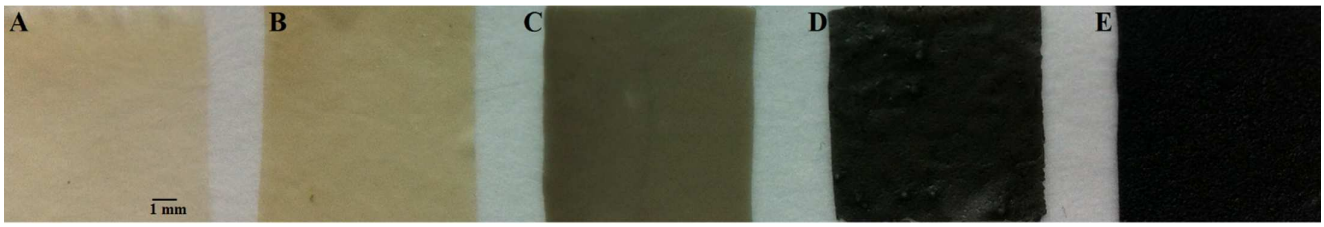

Fig. 3 The photographs of the membranes with different amounts of MWCNTs. A: CP-MIM3 (0%); B: CP/DA-MIM2 (0%); C: CP/CNT/DA-MIM1 (0.5%); D: CP/CNT/DA-MIM2 (1%); E: CP/CNT/DA-MIM3 (1.5%).

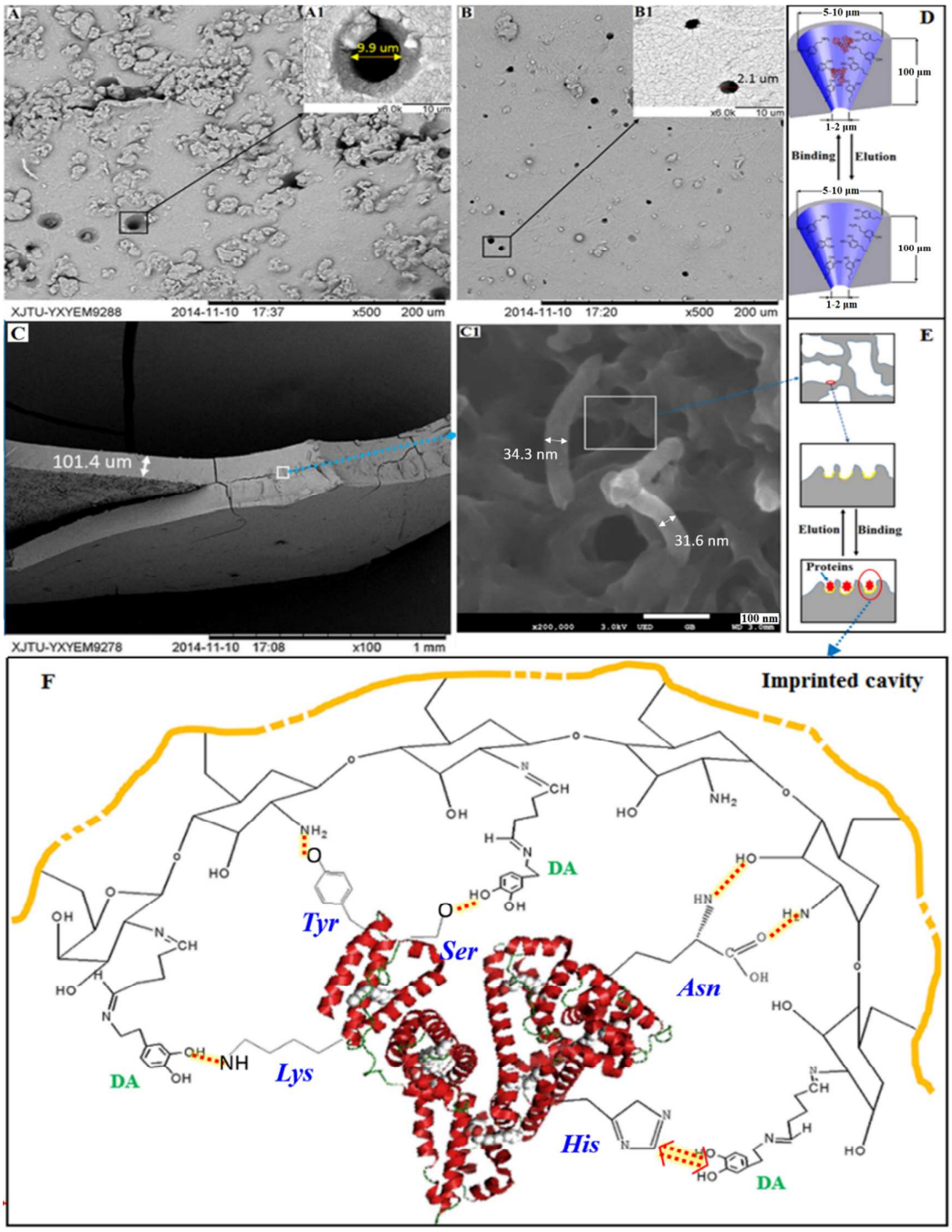

Fig. 4 SEM and FESEM images of the front (A, A1) and back side (B, B1) of CP/CNT/DA-MIM, the cross-section (C, C1) of the membrane with different magnification, the model of funneled thru-hole (D), binding sites (E) and imprinted cavity (F).

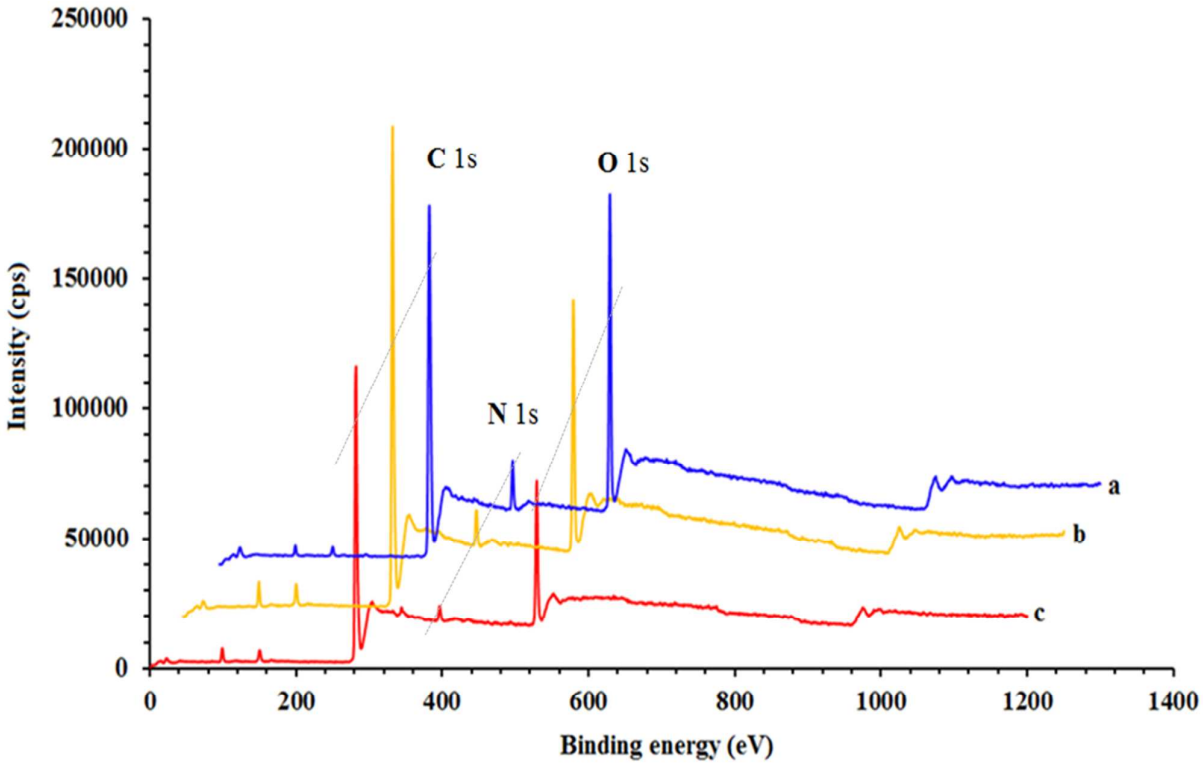

Fig. 5 XPS spectra of CP-MIM (a), CP/CNT-MIM (b) and CP/CNT/DA-MIM (c).

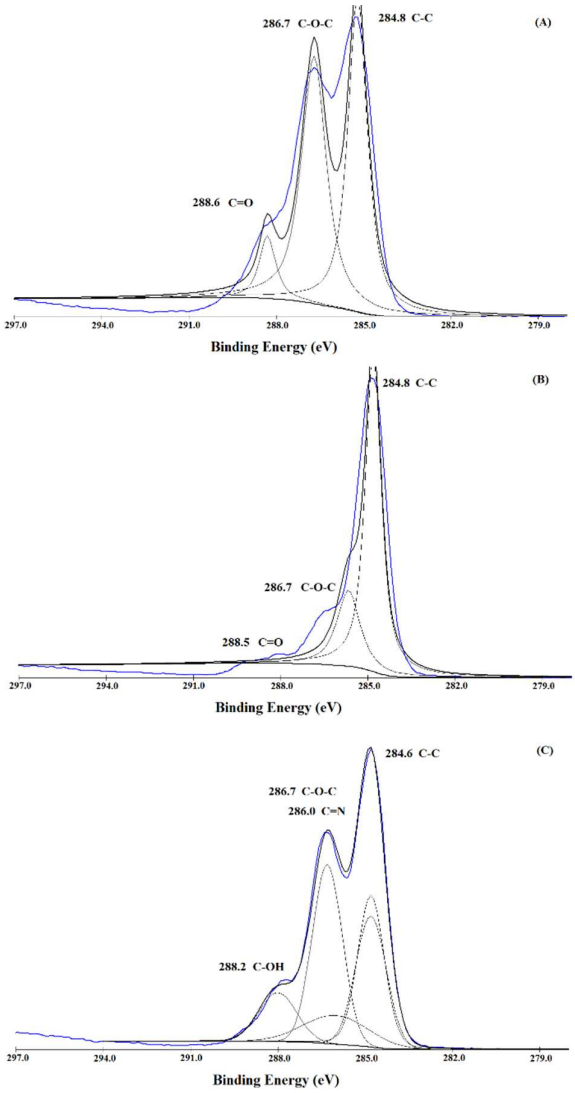

Fig. 6 XPS spectra of C 1s for (A) CP-MIM, (B) CP/CNT-MIM and (C) CP/CNT/DA-MIM.

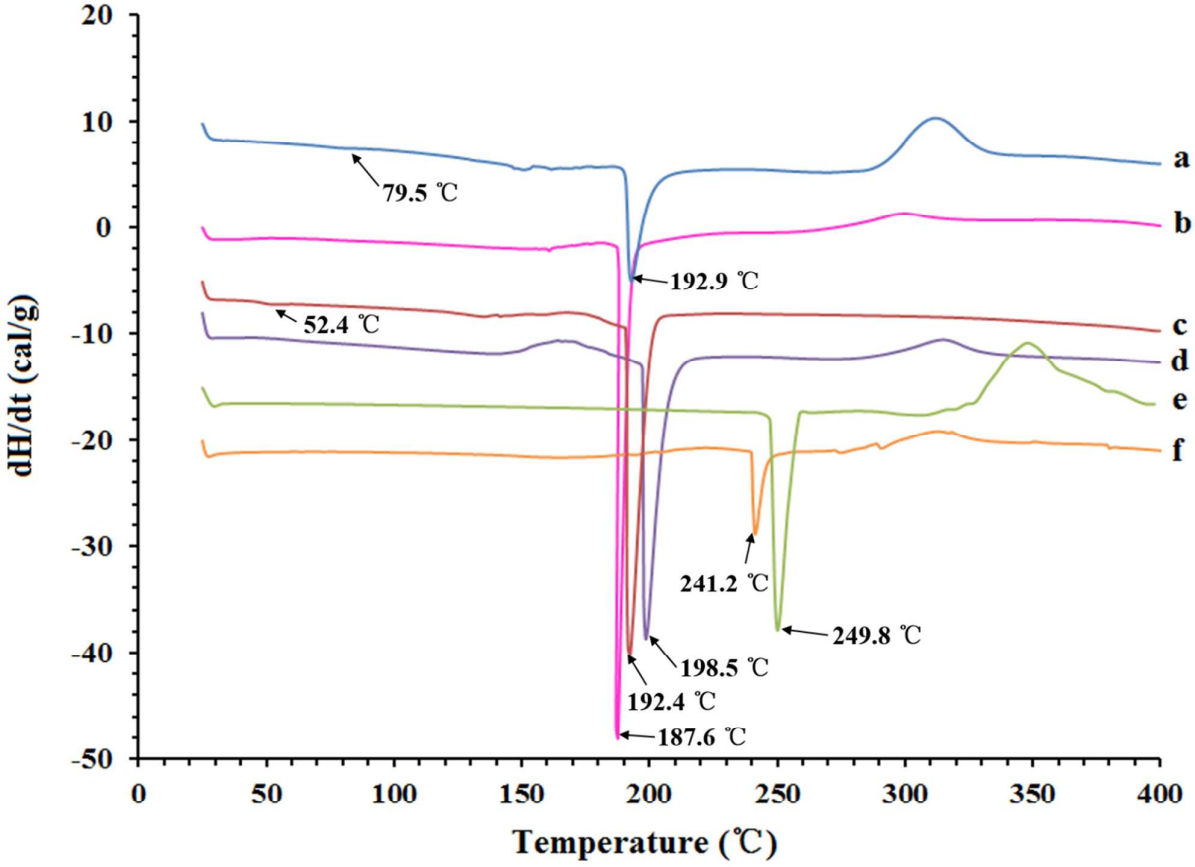

Fig. 7 DSC curves of CS (a), CP-MIM (b), PVP (c), CP/CNT-MIM (d), DA (e), CP/CNT/DA-MIM (f).

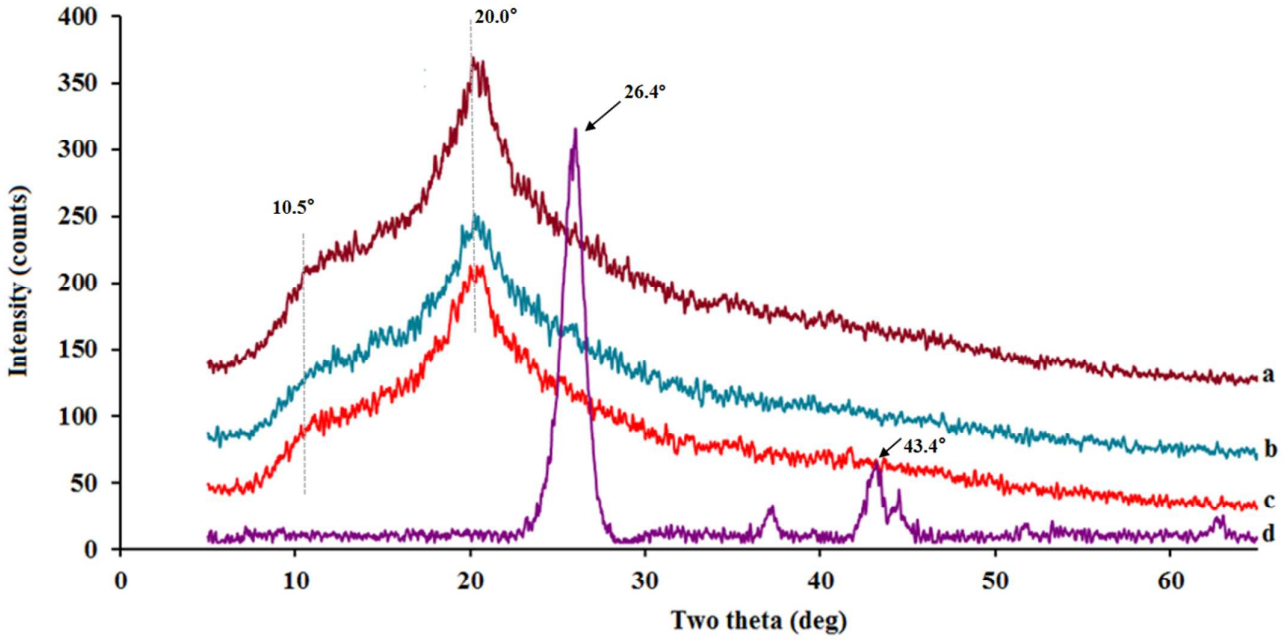

Fig. 8 XRD curves of CP/CNT/DA-MIM (a), CP/CNT-MIM (b), CP/CNT-NIM (c) and virgin MWCNT (d).

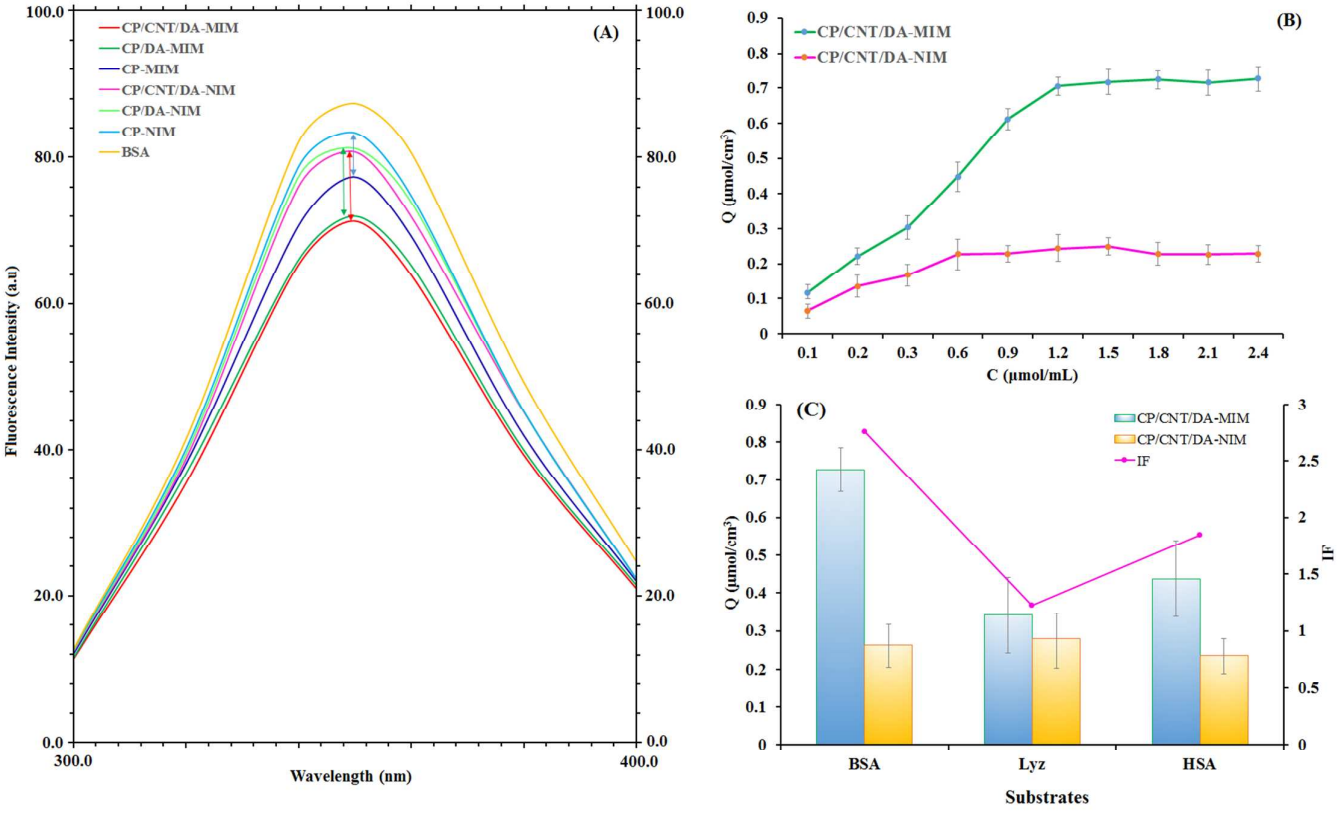

Fig. 9 (A) Fluorescence spectrum of BSA before and after absorbed by different membranes; (B) Adsorption isotherm curves of CP/CNT/DA-MIM and CP/CNT/DA-NIM; (C) Adsorption capacity and imprinted factor of membranes for different substrates.

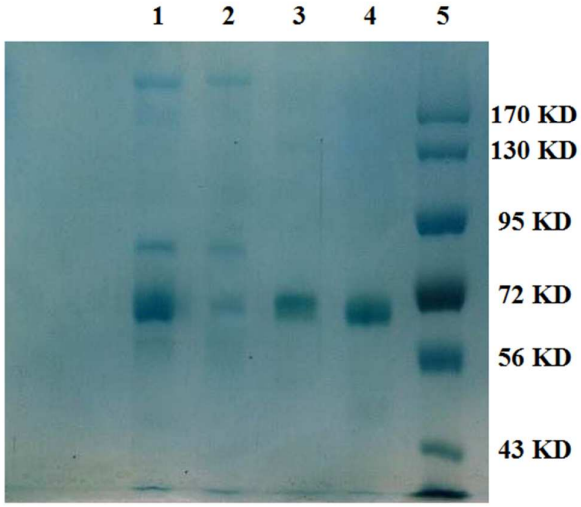

Fig. 10 SDS-PAGE analysis. Lanes 1, bovine blood diluted 100-fold; lanes 2, bovine blood sample (diluted 100-fold) after treated with CP/CNT/DA-MIM; lanes 3, the eluted solution; land 4, 0.25 mg·mL^{-1} of standard BSA solution; lane 5, standard weight molecular protein markers.